Monthly Notices
of the
ROYAL ASTRONOMICAL SOCIETY

Mon. Not. R. Astron. Soc. **417,** 2817–2830 (2011) doi:10.1111/j.1365-2966.2011.19444.x

The properties of brightest cluster galaxies in the Sloan Digital Sky Survey Data Release 6 adaptive matched filter cluster catalogue

A. Pipino,[1,2,3★] T. Szabo,[3] E. Pierpaoli,[3] S. M. MacKenzie[2,4] and F. Dong[5]

[1]*Institute fur Astronomie, ETH Zurich, Wolfgang-Pauli Strasse 27, CH-8093 Zurich, Switzerland*
[2]*Department of Physics and Astronomy, University of California Los Angeles, Los Angeles, CA 90025, USA*
[3]*Department of Physics and Astronomy, University of Southern California, Los Angeles, CA 90089-0740, USA*
[4]*Department of Physics and Astronomy, University of Louisville, Louisville, KY 40292, USA*
[5]*Department of Astrophysical Sciences, Princeton University, Princeton, NJ 08544, USA*

Accepted 2011 July 13. Received 2011 June 14; in original form 2010 November 5

ABSTRACT

We study the properties of brightest cluster galaxies (BCGs) drawn from a catalogue of more than 69 000 clusters in the Sloan Digital Sky Survey (SDSS) Data Release 6 based on the adaptive matched filter technique. Our sample consists of more than 14 300 galaxies in the redshift range 0.1–0.3. We test the catalogue by showing that it includes well-known BCGs which lie in the SDSS footprint. We characterize the Szabo et al. catalogue content in terms of BCGs *r*-band luminosities and optical colours as well as their trends with redshift.

We find that the BCG luminosity distribution is close to a Gaussian with mean −22 mag and dispersion 0.54 mag. The mean has a redshift evolution broadly consistent with pure aging of the galaxies. Richer clusters tend to have brighter BCGs (mean −22.5 mag), however less *dominant* than in poorer systems.

In particular, we define and study the fraction of *blue* BCGs, namely those that are likely to be missed by either colour-based cluster surveys and catalogues, as shown by a direct comparison to maxBCG clusters that are matched in the Szabo et al. catalogue. The overall fraction of blue BCGs goes from ∼5 per cent in the redshift range 0.1–0.2 to ∼10 per cent in the redshift bin 0.2–0.3, with the average over the whole sample of ∼8 per cent. We estimate the possible contamination due to blue outliers at the 1–2 per cent level, while errors on the photometric redshift may lead to an erroneous classification of >0.5 per cent of actual red BCGs as blue. When considering only galaxies with spectroscopic redshift available and for clusters above a richness of 50 – where the catalogue is more than 85 per cent complete – our conservative estimate of the blue fraction is 1–6 per cent (at 99.6 per cent confidence). A preliminary morphological study suggests that the increase in the blue fraction at lower richnesses may have a non-negligible contribution from spiral galaxies.

Finally, we cross-matched our catalogue with the ACCEPT cluster sample, and find that blue BCGs tend to be in clusters with low entropy and short cooling times. That is, the blue light is presumably due to recent star formation associated to gas feeding by cooling flows.

Key words: galaxies: clusters: general – galaxies: elliptical and lenticular, cD – galaxies: evolution – X-rays: galaxies: clusters.

1 INTRODUCTION

The brightest cluster galaxies (BCGs) are the most massive galaxies in the universe, with most of their stellar mass in place by redshift 2. Therefore, they are expected to experience the galaxy formation process in the most extreme way. Namely they should form at earlier times, more rapidly and with a more intense star formation event than lower mass cluster members. While such a formation scenario is naturally explained in the framework of the revised *monolithic collapse models* (e.g. Larson 1974; Pipino, D'Ercole & Matteucci 2008), it seems more difficult to reconcile their existence within the *hierarchical growth scenario* where the largest structures are the last to form. A possible way out is that feedback halted the star formation at very early times and the mass assembly of BCGs can be simply explained with a series of gasless mergers of old stellar

★E-mail: antonio.pipino@phys.ethz.ch

systems (De Lucia & Blaizot 2007; but see Pipino & Matteucci 2008; Whiley et al. 2008; Pipino et al. 2009b). A closer look at their stellar populations tells us that BCGs have similar mean stellar ages and metallicities to non-BCGs ellipticals of the same mass but they have somewhat higher α/Fe ratios, indicating that star formation may have occurred over a shorter time-scale in the BCGs (von der Linden et al. 2007; Loubser et al. 2008). Moreover, they depart from the Faber–Jackson relation for ellipticals (Faber & Jackson 1976) and seem to be larger and with a higher stellar velocity dispersion than ellipticals of the same mass (Bernardi et al. 2007, 2008; von der Linden et al. 2007). Furthermore, the BCG luminosity function differs from the usual Schechter (1976) form that holds for normal cluster members (e.g. Hansen et al. 2005), in that it can be modelled as a Gaussian whose mean increases with the cluster richness (Lin, Mohr & Stanford 2004). Therefore, a study of the colours in BCGs as opposed to 'ordinary' early-type galaxies out to high redshift is a test bench to discriminate among models for galaxy formation (e.g. Roche, Bernardi & Hyde 2010). In particular, the colour evolution may place constraints to the time and the intensity of their last star formation episode, whereas a joint analysis of the colour evolution with the thermal status of the surrounding intracluster medium (ICM) may tell us what halted the gas supply and inhibited further star formation.

Luminous Red Galaxies (LRGs) – as most of the BCGs are – are used as a good tracer of the underlying dark matter distribution (Ho et al. 2009a; Reid & Spergel 2009). Their properties are strongly linked to the host halo mass, so their census can provide us with a map of large-scale overdensities in the Universe. They have been used to detect baryonic acoustic oscillations (see e.g. Sanchez et al. 2009, and references therein), and it has been put forward (Ho, Dedeo & Spergel 2009b) that a combination of a galaxy redshift survey such as Sloan Digital Sky Survey (SDSS) and a cosmic microwave background survey can be used as a method for detecting the missing baryons. Therefore, BCGs can be a promising tool for precision cosmology as well.

Finally, since BCGs occupy a special place in that they sit at the bottom of the cluster potential well, we expect their present-day properties to be linked to the state of the intracluster gas. Recent studies have reported examples of ongoing star formation in the massive central galaxies of cool core clusters (Crawford et al. 1999; Edge 2001; Goto 2005; Hicks & Mushotzky 2005; Edwards et al. 2007, 2009; O'Dea et al. 2008). Bildfell et al. (2008) found that the presence of optical blue cores in 25 per cent of its BCG sample is directly linked to the X-ray excess of the host clusters. Moreover, the position of these BCGs coincides with the peak in X-ray emission. Their interpretation is that the recent star formation in BCGs is associated with the balance between heating and cooling in the ICM in the sense that the clusters that are actively cooling are forming stars in their BCGs. Other evidence comes from Rafferty, McNamara & Nulsen (2008) and Cavagnolo et al. (2008). In particular, Pipino et al. (2009a) demonstrated a one-to-one correspondence between blue cores in BCGs and a UV-enhancement observed using *Galaxy Evolution Explorer* (*GALEX*). The blue light coming from the cores might render the BCGs 0.5–1 mag bluer than the $g - r$ red sequence (Bower, Lucey & Ellis 1992; Baldry et al 2004). This may impact the creation of large optical cluster catalogue based on the presence of a well-defined red sequence as well as on the presence of a BCG.

Szabo et al. (2011) have created the largest available catalogue of optically selected clusters from the SDSS Data Release 6 (DR6). This cluster catalogue is based on the matched filter method (Dong et al. 2008) and does not include any colour selection of member galaxies. An interesting byproduct of the cluster finder algorithm is the creation of the largest available catalogue of BCGs with homogeneous photometry (and photometric redshift) without any selection on colours. In the following, we will refer to the Szabo et al. (2011) cluster catalogue and the related BCG catalogue as synonyms, since each BCG is uniquely associated to a cluster.

The main aim of this paper is to characterize such a catalogue by describing some tests done to check its accuracy, degree of contamination and characterizing the BCG properties in the colour–colour and colour–magnitude spaces. By means of a redshift-independent definition of *blue* BCGs, we will be able to quantify the bias that affects catalogues created via a colour-based selection.

Moreover, with such a BCG catalogue we are in the position of pursuing several main goals. For instance, in this paper we extend the catalogue by including UV–optical colours of the BCGs thanks to GALEX public data. By means of a positional cross-matching of our catalogue with published compilations of X-ray-selected clusters, we are in the position of extending Bildfell et al.(2008) and Pipino et al. (2009a) results to a larger sample of clusters/BCGs.

A quantification of how cooling flows and blue BCGs impact cluster detection from Sunyaev–Zeldovich (SZ) surveys is addressed in a companion paper (Pipino & Pierpaoli 2010).

The scheme of the paper is thus the following. In Section 2 we briefly describe the Szabo et al. cluster catalogue, briefly summarizing the BCGs selection and properties. In Section 3–6 we present the characteristics of the BCG sample in terms of luminosity functions, colours and redshift evolution of these properties as well as we compare them to other existing catalogues. We apply the catalogue to the study of the UV–optical colours and the X-ray properties of our BCGs in Section 7. Conclusions are given in Section 8.

2 THE CATALOGUE

In this section we briefly summarize how the Szabo et al. cluster catalogue that we use has been built. A detailed description can be found elsewhere (Szabo et al. 2011). We also assess the possible contamination of the BCG sample, before proceeding with their characterization.

2.1 Data

The data on which Szabo et al. catalogue has been built are from SDSS DR6 (Adelman-McCarthy et al. 2008). All galaxy measurements were extracted from the *Galaxy* view on the CasJobs DR6 data base.[1] Szabo et al. selected only galaxies that are detected in 1×1 binned images, that have a measurable profile, that are not saturated or contain peaks other than that provided by the estimator of the SDSS pipeline.

The adopted photometric redshifts are based on a neural network CC2 estimator and are available in the table Photoz2 (Oyaizu et al. 2008). We made this choice because of their more reliable error estimates and lack of evident colour biases as opposed to those available from Photoz (Csabai et al. 2003). For more details we refer to Szabo et al. (2011). Absolute magnitudes are calculated by means of the KCORRECTcode v4.1.4 (Blanton & Roweis 2007). In the following, we will always use SDSS *model* magnitudes.

[1] http://cas.sdss.org/dr6

2.2 The cluster catalogue

The matched filter method (Kepner et al. 1999) that Szabo et al. (2011) use is presented in detail by Dong et al (2008). In practice, it is a likelihood method which identifies clusters by convolving the optical galaxy survey with a set of filters based on a modelling of the cluster and field galaxy distributions. A cluster radial surface density profile, a galaxy luminosity function and redshift information (when available) are used to construct filters in position, magnitude and redshift space, from which a cluster likelihood map is generated. The peaks in the map thus correspond to candidate cluster centres where the matches between the survey data and the cluster filters are optimized. The algorithm automatically provides the probability for the detection, best-fitting estimates of cluster properties including redshift, radius and richness, as well as membership assessment for each galaxy. Usage of the apparent magnitudes and the redshift estimates instead of simply searching for projected galaxy overdensities suppresses the foreground–background contamination.

The cluster catalogue is constructed with an iterative procedure. The process starts from a density model of a smooth background with no clusters. For each galaxy position, we then evaluate the likelihood increment we would obtain by assuming that there is in fact a cluster centred on that galaxy. At each iteration, the cluster candidate which resulted in the greatest likelihood increase is retained. A list of cluster candidates then becomes available in decreasing order of detection likelihoods. The cluster richness Λ_{200} is then defined to be the total luminosity in units of L^* inside r_{200}, namely the radius inside which the mass overdensity is 200 times the critical density.

For the magnitude filter, Szabo et al. adopt a luminosity profile described by a central galaxy plus a standard Schechter luminosity function (Schechter 1976).

Dong et al. (2008) showed that the selected cluster sample is ∼85 per cent complete and over 90 per cent pure for systems more massive than $1.0 \times 10^{14}\, h^{-1}\, \mathrm{M}_{\odot}$ ($\Lambda_{200} \sim 50$) with redshifts in the range 0.1–0.4. In order to have a reliable assessment of the BCG colours, we restrict the sample to galaxies in the redshift range [0.1, 0.3], where the intrinsic scatter in the observed $g - r$ colour is the smallest. The estimated cluster redshifts derived from maximum likelihood analysis show small errors with $\Delta z < 0.01$.

The final Szabo et al. catalogue has more than 69 000 entries. We refer the reader to the main catalogue paper for details on the cluster characteristics and comparison with other automated catalogues. A complete version of the catalogue with the three brightest galaxies from which we derive the sample discussed in this paper can be found in Szabo et al. (2011).

2.3 The final BCG sample

We will focus on BCG as the brightest[2] member in every group or cluster of galaxies in the r band. We further exclude from the analysis galaxies whose error on the $g - r$ colour, expressed as $3\sqrt{\sigma_g^2 + \sigma_r^2}$, exceeds 0.3 mag. They represent about less than 1 per cent of the galaxies in the redshift range 0.1–0.3. The final sample comprises of 14 344 galaxies.

The number of BCGs (Fig. 1) increases with redshift as the underlying cluster redshift distribution. The richness of the cluster does not play a role: the histogram for rich clusters tracks the one for the whole population.

[2] As opposed to other selection criteria such as being the highest likelihood member or the closest to the estimated cluster centre.

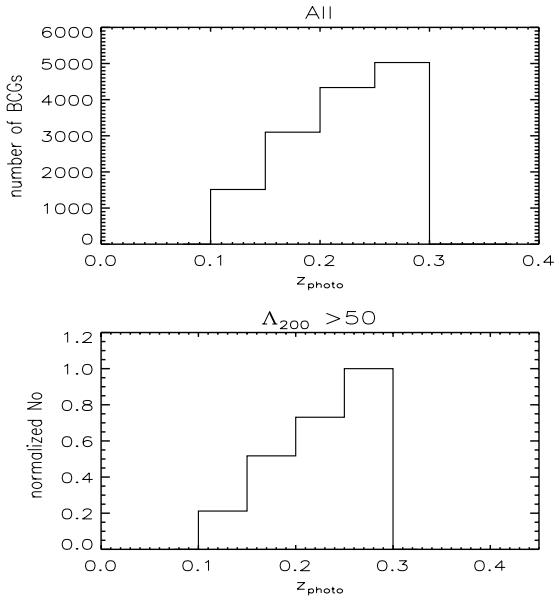

Figure 1. Redshift distribution of all the BCGs and those in rich clusters.

2.4 A test of the accuracy of the catalogue: matching known BCGs

We tested the accuracy of our selection by cross-matching the position of such an extended BCG sample with known coordinates of well-studied BCGs taken from the literature (Crawford et al. 1999; Bildfell et al. 2008; Loubser et al. 2008, as well as the SIMBAD data base) whose position is within the region of sky covered by SDSS DR6 and that lie at $0.1 < z < 0.3$. While we will mostly focus on BCG as the 'brightest' member in every group or cluster of galaxies, it is important to consider also the second and third most luminous galaxies in a cluster (by using the r-band magnitude luminosities) in the following exercise. This is needed because the above mentioned works either defined the BCG as the brightest galaxy in a band other than the r one or by their position in the cluster. Therefore, there are a few cases in which their BCG is either the second or the third brightest in our definition.

Our sample matches 73 per cent of the BCGs in the Crawford et al. (1999) list with an accuracy of less than 0.3 arcsec in angular position and of less than 0.01 in redshift space, and more than 80 per cent with if we require an accuracy of a few arcseconds, which is the typical error in the coordinates. Also differences in coordinates among authors (and the SIMBAD data base) for the same galaxy may amount to a few arcseconds.

In the remaining 20 per cent of the cases, (i) the known BCG that we want to match lies too close to the edge of the sky region covered by the SDSS DR6 and the adaptive matched filter (AMF) finder has problems in identifying a cluster there, (ii) it is very close to the limit redshift range considered in this work; as an example we mention the case when the BCG to be matched has redshift 0.1, but its host cluster has a redshift < 0.1 and falls in the region where our catalogue is not complete (and thus missed) and (iii) it is part of a substructure of a bigger cluster that it is not *resolved* by our cluster finder.

A further complication is that, in the above mentioned literature compilations, the authors often *decide* which galaxy to label as the BCG when galaxies with very similar luminosity were present.

In some cases, their selection has been done on the basis of the presence of an extended stellar halo which clearly made the BCG candidate a cD galaxy. In other cases, the galaxy closer to the X-ray centre of the cluster has been selected. Finally, there are cases in which a galaxy cluster is made of subclusters in the act of merging, each one with its own BCG. Therefore, it is not surprising that we have a fraction of cases in which the positional best match with a known BCG has been obtained by the second or the third most luminous galaxies in the entire Szabo et al. BCG sample. Also, we have cases in which the first and the second brightest galaxies of a given cluster in our entire BCG sample match the BCGs of two known (merging) subclusters.

Other works (e.g. Koester et al. 2007) return a similar success rate. In colour-based finding methods, the known BCGs that are not matched typically feature emission lines and are possibly offset from the red sequence (Koester et al. 2007).

3 THE BLUE FRACTION AND THE PURITY OF THE CATALOGUE

The following BCG characterization relies on photometric redshifts. The cluster finder method is not based on the red sequence, therefore it is not biased against the presence of BCGs with unusual colours. On the other hand, it is important to assess whether a contamination of background/foreground galaxies with 'unusual' colours biases the sample. In particular, it is important to define and characterize the fraction of *blue* BCGs. In this work, galaxies 0.3 mag below (i.e. bluer than) the average $g - r$ colour (observed frame) for early types at their respective redshifts are considered as blue BCGs. Since these galaxies obey the colour–magnitude sequence, and since we focus on a narrow range in luminosities (at the high-mass/luminosity end), in practice our requirement implies that these blue BCGs will lie below the red sequence at their given redshift. Indeed, we chose such a cut-off since 0.3 mag is more than 6σ off the mean value of the colour–magnitude relation (Bower et al. 1992). In practice, we self-consistently evaluate the average $g - r$ at a given redshift by means of our BCG sample, and we use it as a zero-point for measuring the offset (i.e. the blueness) of the single galaxies. Not surprisingly, it turns out that this coincides with the mean trend of the $g - r$ versus redshift curve reported by Blanton & Roweis (2007; cf. their fig. 3), hence basically with the locus where galaxies in the Cut I subsample of the luminous red galaxy (LRG) sample (Eisenstein et al. 2001) lie. In other words, it is very likely that LRGs that are also BCGs in their own cluster end up as BCGs in the Szabo et al. catalogue. The converse is not true, since the colour cuts in the LRG sample get rid of the galaxies that, albeit very bright, are 0.3 mag bluer than the average $g - r$ colour. The fraction of the galaxies bluer than the average with respect to the total number of BCGs gives us an estimate of the colour bias – possibly introduced by recent star formation (and cooling flows) – into red-sequence-based cluster catalogues.

In Fig. 2 we show the $g - r$ colour as a function of photometric redshift for all BCGs (top panel), whereas we focus on those in rich cluster in the bottom panel. We note a clear asymmetry in that the number of BCGs 0.3 mag bluer (brighter points) than our cut-off, which is roughly given by the relation $g - r \sim 2.86z + 0.35$ (solid line), is larger than that of the galaxies on the red side of the average sequence ($g - r \sim 2.86z + 0.65$, dashed lines).

In order to guide the eye, we also plot – bracketed by lighter dashed lines – the 1σ region around the mean relation found by Koester et al. (2007) for their BCGs (cf. their fig. 2) which follow more closely the mean red-sequence evolution as a function of redshift. On the other hand, the bulk of our BCGs in clusters of richness above 50 matches very well the relation for red and dead early-type galaxies. A number of blue outliers are still present though. We further discuss these galaxies below.

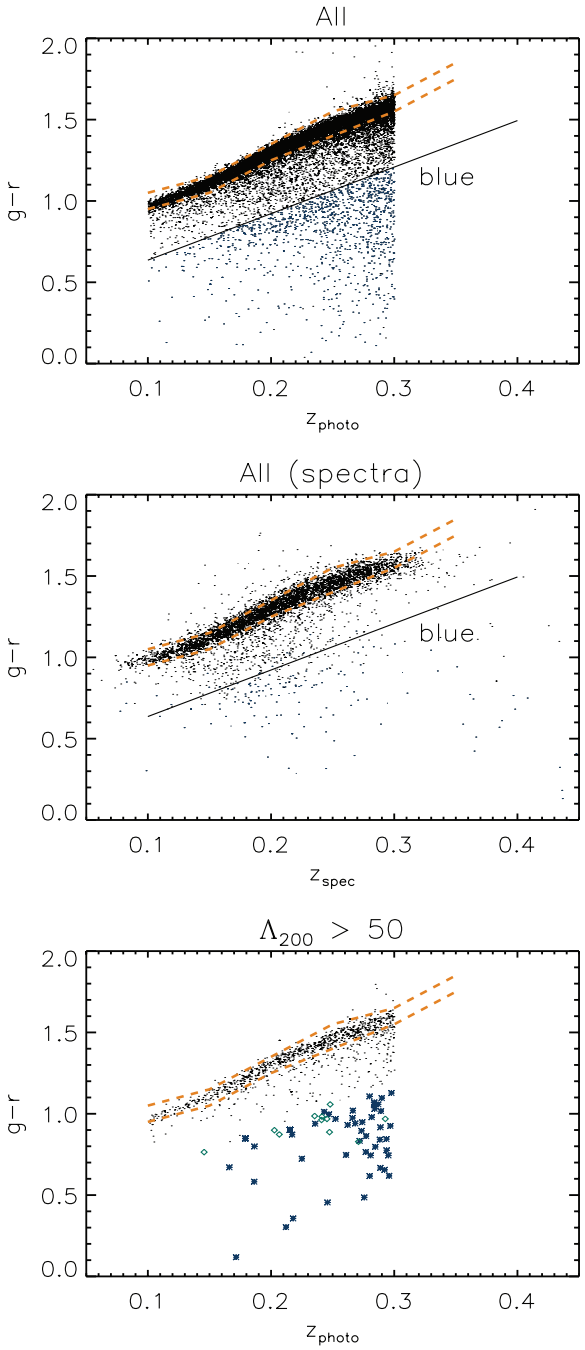

Figure 2. $g - r$ colour as a function of photometric and spectroscopic redshift for all BCGs (top and middle panels, respectively). $g - r$ colour as a function of photometric redshift for those in rich clusters (bottom panel). BCGs bluer than 0.3 mag from the red sequence at their redshift (i.e. below the solid line, in the 'blue' region) are presented by means of brighter points. We also highlight them using the asterisk symbols in the panel for high richness clusters, whereas squares highlight spirals. Dashed lines: 1σ region around the mean relation found by Koester et al. (2007) for their BCGs (their fig. 2, see also Blanton & Roweis 2007).

3.1 The blue fraction in the Szabo et al. catalogue

We now quantify the fraction of blue BCGs in the Szabo et al. catalogue. This value gives an upper limit to the intrinsic blue fraction in BCGs and can be considered as a qualitative characterization of the cluster content for users not interested in further details on the galaxies. In Fig. 3 we show the distribution in the offset in magnitudes from the average $g - r$ in different redshift slices. Whilst the large majority of BCGs display a negligible offset and follow the same trend of the LRGs studied by Blanton & Roweis (2007), the histograms show a clear tail on the blue side (positive *offset* in our figures). As expected from Fig. 2, there is a clear asymmetry in the number of BCGs bluer than the red sequence, with respect to those redder. Note, however, that the curves become more symmetric and the relevance of the blue BCGs diminishes if we take into account only rich clusters (see also e.g. Skibba 2009) and as we move to lower redshift. In particular, we find that the overall fraction of first ranked galaxies bluer than 0.3 mag is 8.7 per cent [8.1–9.5 per cent is the 99.6 per cent confidence interval calculated by using the Beta distribution for binomial populations (Cameron 2011)]. Such a fraction slightly decreases to 6.5 per cent (5.6–7.6 per cent) if we restrict ourselves to clusters with richness above 30, and decreases to the 6.1 per cent (4.4–8.5 per cent) above a richness of 50. For comparison, the blue fraction of all cluster members in the same redshift range is 20.6 per cent (20.4–20.9 per cent). In terms of redshift bins, the blue fraction goes from 4.7 per cent (3.8–5.7 per cent) in the redshift range 0.1–0.2 to 10.7 per cent (9.8–11.7 per cent) in the redshift bin 0.2–0.3. Thus blue BCGs tend to populate poor clusters and their fraction slightly increases with redshift. Note that at higher redshifts both the scatter in the $g - r$ colour and its error tend to increase.

To better quantify if the blue population is due to background contamination, we further computed the number of possible contaminants in the direction of our clusters and compared it to the average number density of blue galaxies. Fig. 4 shows the results for the analysis done on stripe 10. In practice, we took all the $\sim 2 \times 10^6$ galaxies in that stripe used as input to construct the Szabo et al. catalogue. We classified them as blue and red, according to the photometric redshift, as done for the BCGs. We computed the average number density of the blue objects, brighter than $r = 20$, per arcmin^2 in the whole stripe. We find 0.022 arcmin^{-2} for $z = [0.1,0.15]$, 0.025 arcmin^{-2} for $z = [0.15,0.2]$, 0.024 arcmin^{-2} for $z = [0.2,0.25]$ and 0.019 arcmin^{-2} for $z = [0.25,0.3]$. Based on these numbers, we would expect a $\sim$2 per cent of finding a bright blue object in the centre of a detected clusters in a suitable redshift slice. We use this number as our estimate of the average probability of contamination over the whole stripe. We then looked for an excess of blue objects brighter than 20 mag in the r band in a deg^2 in the direction of each cluster detected in that stripe, in a redshift slice $\delta z = 0.05$. The number densities of contaminants (i.e. blue objects including the BCG itself, if blue) as a function of the BCG magnitude and BCG colour are shown in Fig. 4. The scatter in the number of possible outliers is lower around blue BCGs than around red BCGs. However, the mean densities (0.022 arcmin^{-2}) are similar and equal to the average over the whole stripe. If one looks at galaxies brighter than the

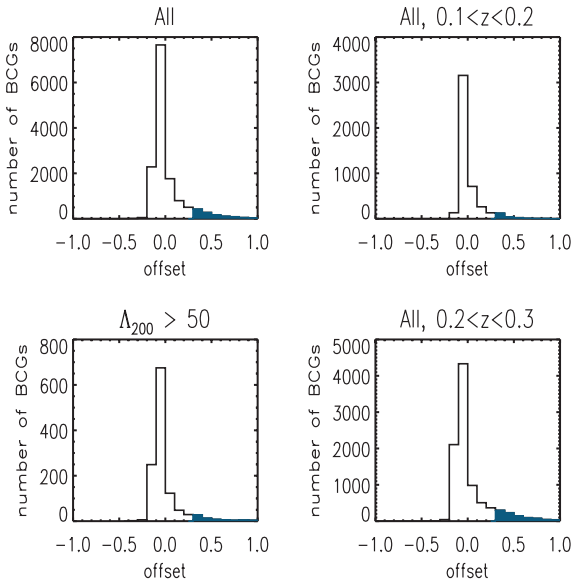

Figure 3. Offset (mag) from $g - r$ colour–magnitude relation as a function of richness and offset distribution in redshift slices. The shaded area emphasizes the tail of blue BCGs.

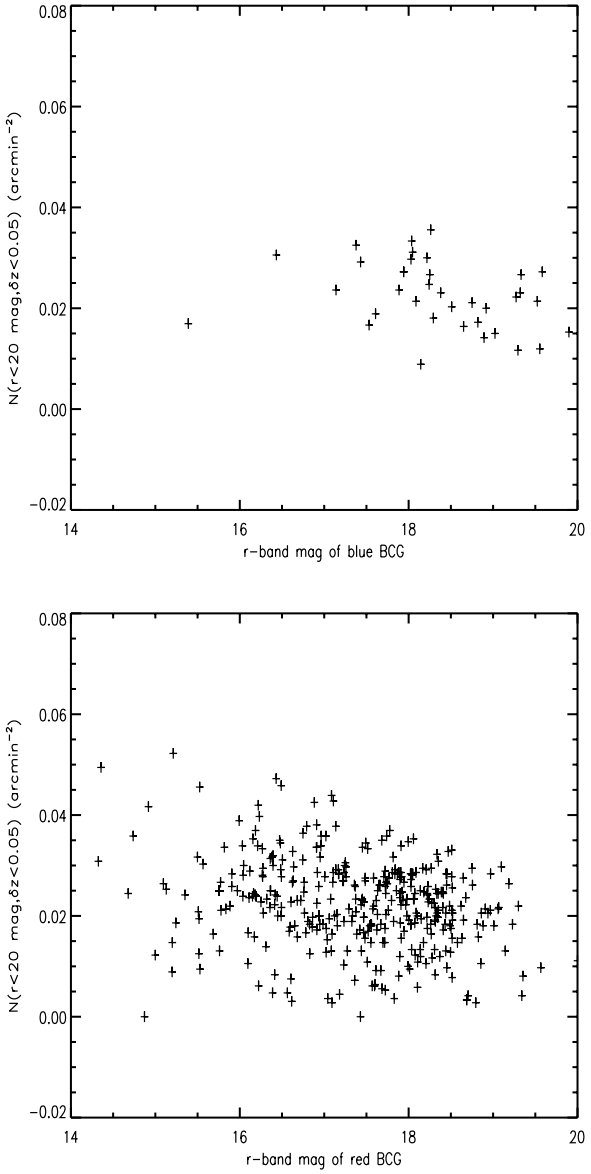

Figure 4. Number of blue objects brighter than 20 mag arcmin^{-2} in the direction of the clusters in a redshift slice $\delta z = 0.05$ as a function of the BCG magnitude. The two panels are for red and blue BCGs.

BCGs, the number densities further decrease and are comparable to the average one only at the very faint magnitudes $r > 19$ and at $z \sim 0.3$ (not shown here). We do not detect any enhanced overdensity of blue contaminants in the background of clusters hosting a blue BCG with respect to those harbouring red ones that may be symptom of a contamination. Given the above densities, we estimate the background contribution to the blue population at most at 2 per cent level in the entire sample, namely smaller than the estimated blue fraction. This number agrees with the estimated projection effect for the entire population in that stripe. It is also consistent with the overall contamination estimate given in the parent catalogue. By studying the error induced in the host cluster redshifts by means of photometric redshift, Szabo et al. (2011, table 4) estimate that at most 1 per cent of the BCGs in the redshift range studied here are indeed projected.

A common colour cut used to discriminate between early-type morphologies (which BCGs belong to) from later type at $u - r > 2.22$ has been derived by Strateva et al. (2001) on an earlier release of the SDSS. This requirement is satisfied by the 95 per cent of our BCGs in clusters with richness above 30, in agreement with Strateva et al. (2001), who found that 97.6 per cent of their (spectroscopically classified) early-type galaxies were above the $u - r = 2.2$ threshold. On the other hand, only 42/3333, namely the 12.6 per cent (with 8 per cent – 18.8 per cent bracketing the 99.6 per cent confidence interval) of those that are blue according to our classification make this threshold. In agreement with us, Choi, Park & Vogeley (2007) found that about 10 per cent of early-type galaxies with evidences of a blue optical core in a volume-limited sample of SDSS have a $u - r$ colour bluer than 2.22. Most of these galaxies live in low-density environment as we found. Unfortunately, a cross-match with their catalogue is impossible because it does not overlap in redshift with ours, theirs being at redshift below 0.1.

3.2 The blue fraction in galaxies with spectra

The fraction of blue BCGs in the whole sample goes down to 3.7 per cent when considering only the galaxies that have a spectroscopic redshift (middle panel of Fig. 2). We have spectroscopic redshifts for just one-third (5642/14 344) of the BCGs in the range studied. In particular, the fraction of blue BCGs in clusters with richness above 50 that have a spectroscopic redshift decreases to a few per cent as we discuss below. In this latter case, all the galaxies with $g - r < 0.7$ would disappear from the lower panel in Fig. 2 and their fraction is strongly suppressed in the entire sample (compare the middle panel to the upper panel). This may be a symptom that a fraction of the blue BCGs for which we have only photometric redshift is not physically associated to their host cluster, despite the contamination estimated above is relatively low (∼2 per cent). In order to shed light on this issue, we now compare in detail the blue fraction for galaxies with and without spectroscopic redshift.

Let us start with testing the impact of photometric redshifts on the blue fraction. We define two subsamples of BCGs either with or without spectroscopic redshift, but with the same richness ($\Lambda > 50$) and apparent magnitude ($r < 18$) cuts. In practice, such a selection yields a sample of ∼350 galaxies with spectroscopic redshift. We randomly selected other 350 without spectroscopic redshift in the same richness and magnitude range. The former sample yields a blue fraction of $0.020^{0.05}_{0.006}$ (99.6 per cent confidence level), whereas the latter gives $0.042^{0.08}_{0.018}$. The two values differ by a factor of 2, but they are consistent within (less than) 3σ, and we cannot exclude that spectra were preferentially taken for galaxies sitting

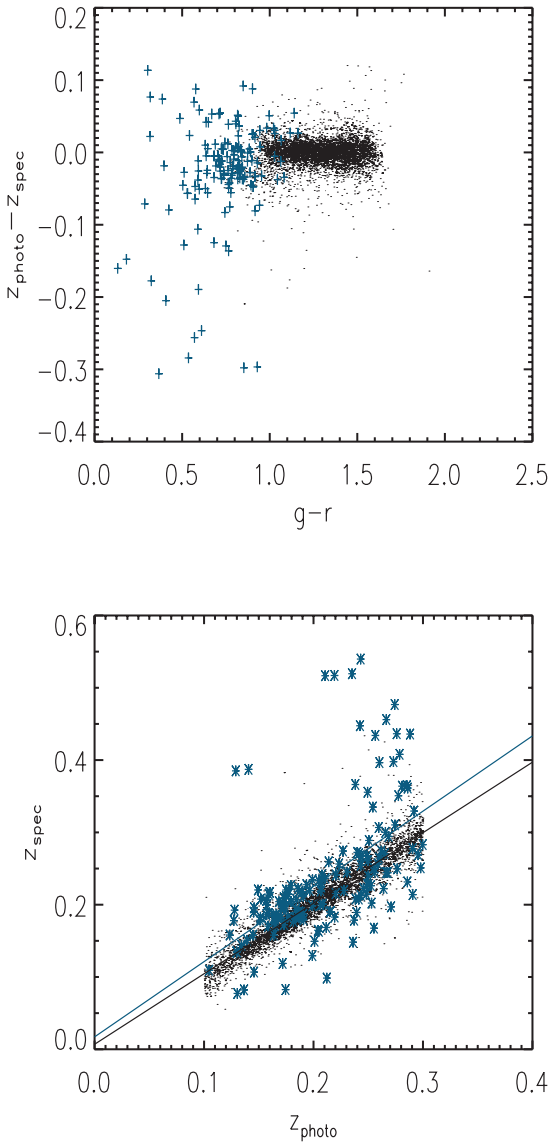

Figure 5. Top: difference in the photometric and the spectroscopic redshift (when available) as a function of the $g - r$ colour for the BCGs in the Szabo et al. catalogue (blue BCGs are highlighted with larger symbols). Bottom: photometric versus spectroscopic redshift for the BCGs studied in this paper. The blue BCGs (see text) are highlighted with lighter asterisks. Linear fits to the data are provided as solid lines.

on the red sequence, hence artificially removing blue galaxies. A close inspection to galaxies in rich clusters tells us that, while the difference between spectroscopic and photometric redshift tends to be very small (<0.02) in red galaxies, it is not uncommon to find 'blue' galaxies whose spectroscopic redshift is 0.1 lower than the photometric estimate. Given the quite steep variation of $(g - r)$ with redshift (cf. Fig. 2), such a galaxy might be perfectly on the red sequence when the correct (spectroscopic) redshift is used. To better illustrate the issue, in Fig. 5 (bottom panel) we plot the spectroscopic redshift versus the photometric one for the subsample of BCGs on which we focus in this paper. Almost 90 per cent (4768/5304) of the BCGs have a difference between spectroscopic and photometric redshift smaller than 0.03. The fraction is nearly 60 per cent (78/133) when blue BCGs are considered. A linear fit to the relations shows

that, while the correlation is 1:1 for the entire sample of BCGs (solid black line in Fig. 5, lower panel), photometric redshift (blue line in Fig. 5, lower panel) tends to slightly underestimate the distance for galaxies that we would define as blue in the $(g - r)$–photometric redshift plane. This is true also when we compare the BCG redshift to the cluster redshift (Szabo et al. 2011, fig. 9), with a systematic mean offset of 0.015.

In particular, out of 159 blue BCGs (any richness) with spectroscopic redshift available, 44 of them (27.7 per cent) have $\mathrm{abs}(z_{\mathrm{photo}} - z_{\mathrm{spec}}) > 0.05$. 15 of these have $z_{\mathrm{photo}} - z_{\mathrm{spec}} > 0.05$: they can be erroneously classified as blue. 9/15 are red according to the spectroscopic redshift. As for the other 29, using the spectroscopic redshift will put them farther away (for 22/29, $z_{\mathrm{spec}} > 0.3$) and if they are blue according to their photometric redshift, they will be 'even bluer' at their spectroscopic one.

It is important to stress that in all cases discussed above, the host cluster's redshift almost coincides with z_{spec}, because spectroscopic redshifts of the BCG and/or of other cluster members weight much more than the photometric ones in the cluster redshift determination (Szabo et al. 2011, fig. 9). Therefore, these galaxies are not 'background/foreground' contaminant in a strict sense: 9/159 (5.7 per cent) of blue BCGs are indeed red according to their spectroscopic (and/or cluster's) redshift. Assuming that this fraction of erroneously determined blue BCGs applies to the entire sample, we can estimate that 5.7×8.7 per cent ($\sim$0.5 per cent) of the BCGs in our entire sample are erroneously classified as blue because of the use of the photometric redshift instead of the spectroscopic one in the $(g - r)$–redshift plane and not because the allegedly blue BCG is a foreground/background object, that we incorrectly classify as a cluster member.

If we create a catalogue of BCG whose cluster's redshift is in the range 0.1–0.3, we find a somewhat smaller number of entries (12 753), but the blue fraction is the same (8.7 per cent). This means that, although a few single galaxies can scatter in/out of our predefined redshift range, these fluxes compensate each other and yield an overall robust blue fraction.

Finally, in Fig. 5 (upper panel) we show the difference in the photometric and the spectroscopic redshift (when available) as a function of the $g - r$ colour for the BCGs in the *input* Szabo et al. catalogue. Despite outliers are present, no clear bias with colour is found. We thus infer that the classification of a BCG as a blue object might be biased by errors in the photometric redshift, whereas the $g - r$ colour does not bias the measure of the redshift.

In conclusion, even considering the *overall* accuracy of state-of-the-art photometric redshifts estimates, we cannot exclude that a fraction of the bright blue BCGs are so because of the *specific* error in their photometric redshift.

Less bright ($r > 18$ mag) blue BCGs tend not to have spectroscopic redshift against which we can compare the photometric estimates. Moreover, the input catalogue features an increase in the blue fraction with decreasing richness. Some of the poorest groups in the catalogue may be either loose associations of predominantly faint blue galaxies (see also below for morphologies) or artefacts. Therefore, we recommend to limit the study to galaxies in clusters with $\Lambda_{200} > 50$.

Using only galaxies with spectra, a conservative final estimate of the blue fraction of BCGs in the redshift range 0.1–0.3, at richnesses above 50, is 2 per cent (0.6–5.2 per cent at 99.6 per cent confidence). Such estimate is in agreement with the results of Edwards et al. (2007), who selected BCGs by means of K-band magnitudes and found that $\sim$3 per cent of those had bluer $u - r$ colour than expected.

3.3 A visual morphological inspection

Until this point, we did not take into account the morphology of the BCGs. However, it is important to assess whether the blue BCGs are truly early-type galaxies or if the sample is contaminated by late-type (i.e. bluer star-forming) galaxies. These may be identified as BCGs if sufficiently bright members of clusters lack, e.g., a well-defined red sequence or a prominent early-type central galaxy. In particular, for application to galaxy formation studies, it can be worthwhile investigating if the blue fraction is due to a contamination from other galaxy types as opposed to elliptical ones. For instance, lenticular galaxies are BCGs in known clusters, while spiral galaxies may dominate groups.[3]

At this stage, we used a visual inspection of SDSS images in order to coarsely divide the sample into (i) ellipticals, (ii) ellipticals/interacting (which include also galaxies of elliptical shape in dense regions that overlap on the line of sight, although not necessarily physically bound); (iii) spirals and (iv) unknown. When the spectra were available, we also checked the presence of emission lines.

In the richest ($\Lambda_{200} > 100$) clusters of our sample, 93 per cent of the galaxies are single or interacting ellipticals, the rest being 'uncertain' according to this preliminary visual morphological classification. In particular, the interacting ellipticals alone amount to 34 per cent, similar to what found for $z \sim 0$ massive ellipticals by Kannappan, Guie & Baker (2009). According to Kannappan et al. (2009), these galaxies populate low to moderate density environments. We found that the distributions of these interacting early-type galaxies around the average $g - r$ colour at a given redshift and in absolute magnitude are very similar to the one that single ellipticals exhibit. For the above reasons, we suggest a cut at $\Lambda_{200} > 100$ for studies focussing on red *early-type* BCGs in massive galaxy clusters.

In order to study potential contamination, we further visually inspected all the blue BCGs in $\Lambda_{200} > 50$ clusters of our sample. Among them, the percentage of ellipticals decreases to 70 per cent. 5 per cent of these blue galaxies are indeed spirals typically associated to $\Lambda_{200} \sim 50$ clusters (squares in Fig. 2). This number might be seen as a upper limit to the contamination of our BCG sample. However, we cannot exclude that a sizable fraction of these spirals are indeed members of relatively poor systems and not outliers. Being associated to poorer systems, these spirals are on average fainter. Therefore, we suggest a cut at $M_r < -22.5$ if one wants to use a sample almost made by BCGs that are early-type galaxies. The morphology-richness trend seems to follow the increase in the blue fraction at lower richness that we discussed above. It is worth noting that similar findings are also reported by other studies of the correlation between BCG properties and cluster mass. For instance, More et al. (2011), using the kinematics of satellite galaxies to infer the halo mass, found that, at a given galaxy luminosity, red central galaxies tend to occupy more massive haloes than the blue ones. Similar results are reported by Loh et al. (2010) by means of the two-point correlation function as well as the NUV $-$ r colours. These independent results have been obtained below $z \sim 0.1$, therefore we can confirm the reported trends and extend their validity out to $z = 0.3$.

[3] It is worth reminding the reader that relation between Λ_{200} and the cluster mass has a substantial scatter below $\Lambda_{200} = 50$ (fig. 6 in Dong et al. 2008), such that $\sim 2 \times 10^{14}\, h^{-1}\, \mathrm{M}_{\odot}$ poor clusters and $\sim 5 \times 10^{13}\, h^{-1}\, \mathrm{M}_{\odot}$ groups can be assigned the same richness.

A more detailed study on the morphologies in the Szabo et al. catalogue is underway (MacKenzie et al., in preparation).

4 BCG CHARACTERIZATION

In this section we will focus on the BCG characterization in terms of luminosity, and explain how the inclusion of *blue* BCGs makes the Szabo et al. (2011) catalogue different from others in the literature. For a comparison of BCG luminosity distributions between catalogues, we refer to Szabo et al. (2011).

4.1 BCG luminosity

In Fig. 6, we compare our BCGs to the BCG magnitude–redshift relation inferred by Loh & Strauss (2006) for LRG in the redshift range 0.12–0.38. The dashed lines bracket the 1σ scatter around this relation. At high richnesses (lower panel), the spread in our BCG sample is comparable with a $\sim 3\sigma$ scatter around Loh & Strauss relation, as well as the mean trends look very similar to each other. In particular, we find that $r \sim 12.6z + 14.7$. A substantial population of blue BCGs is present when considering the entire sample (upper panel), and offsets our distribution towards fainter magnitudes with respect to Loh & Strauss (2006) findings.

In Fig. 7 (upper panel) we show the distribution in luminosity in the r-band for the BCGs in the redshift range [0.1, 0.3] as a thick solid line. This curve is well approximated by a Gaussian distribution with mean equal to the average M_r in the same redshift range and $\sigma \sim 0.5$ mag which is commonly adopted as the BCG luminosity function (e.g. Hansen et al. 2005). Also highlighted (lower panel) are the distribution functions in clusters with richness above 50. We find that the mean magnitude is -22.06 (-22.50 in the richest clusters), with $\sigma = 0.544$ mag (0.5 for rich clusters). We have seen that bluer BCG tends to populate poorer systems. Since the BCG luminosity scales with the cluster richness (Lin & Mohr 2004; Hansen et al. 2009; see also table 5 in Szabo et al. 2011), blue BCGs (dashed line) tend to be fainter (median magnitude is -21.67) and more broadly distributed ($\sigma = 0.7$ mag) than the average.

The median M_r slightly increases (conversely the luminosity decreases) at smaller redshift: from -22.06 for $z = [0.2,0.3]$ to -21.95 for $z = [0.1,0.2]$, namely the average luminosity drops by $\sim$20 per cent from redshift 0.3 to 0.1. Such a change is consistent with that expected from pure passive evolution (e.g. Tinsley 1980; Nelson et al. 2001). The increase is less evident when looking at the high-richness cluster, being only 0.04 mag. The dispersion slightly increases with decreasing redshift, being 0.56 mag for the entire sample (0.55 for rich clusters) at $z = [0.1, 0.2]$ and 0.53 mag (0.48) in the higher redshift bin.

A comparison between the two panels makes evident that the tail at faint magnitudes is due to BCGs in low-richness clusters. A more quantitative assessment of the BCG luminosity function and its evolution would require a more careful treatment of the data. Here we rely on the absolute magnitude in the r band calculated by means of the template fitting approach (Csabai et al. 2003; Blanton & Roweis 2007) but with photometric redshift derived from a neural network estimator (Oyaizu et al. 2008), namely not in a self-consistent way. Furthermore, no evolutionary corrections have been applied. Moreover, it is known that sky subtraction errors in the SDSS pipeline may significantly affect the magnitude of the brightest objects (see Adelman-McCarthy et al. 2008, and references therein). In addition, the catalogue is not complete at the poor-richness end, and this implies that the low-luminosity tail of the luminosity distribution is not correctly represented. Finally, the effect of small number statistics is clear in the distribution for rich ($\Lambda_{200} > 50$) cluster.

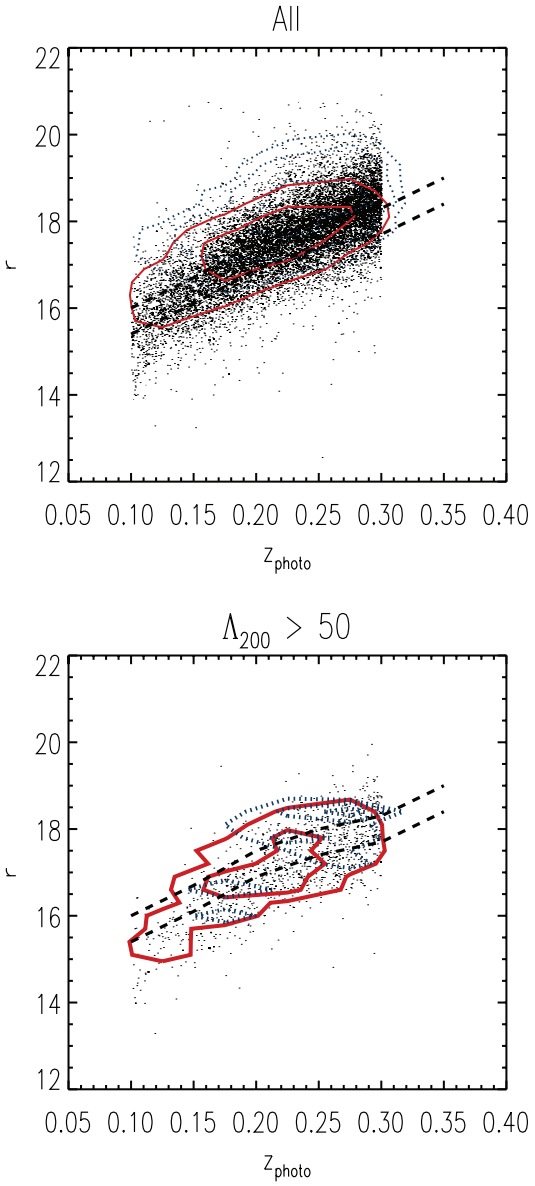

Figure 6. Distribution of galaxies in the plane r-band magnitude versus photometric redshift: all BCG (points and solid contours, upper panel) and galaxies in clusters with richness larger than 50 (solid contours, lower panel). BCGs bluer than 0.3 mag from the red sequence at their redshift are shown by dotted isodensity (number of galaxy/bin area) contours. Dashed lines: 1σ region around the mean relation by Loh & Strauss (2006) for BCGs in SDSS. Compare with fig. 3 of Koester et al (2007).

In concluding the section, we add that Fig. 7 suggests a cut at $M_r < -22.5$ if one wants to use a sample almost made by red BCGs.

5 THE BCG DOMINANCE

In this section we compare the properties of the brightest galaxy to the second and the third brightest ones.

In particular, we express the *dominance* in terms of the difference in r-band apparent magnitude $r_{2nd} - r_{1st}$ between the second and the first ranked galaxies. The distribution of the values is shown

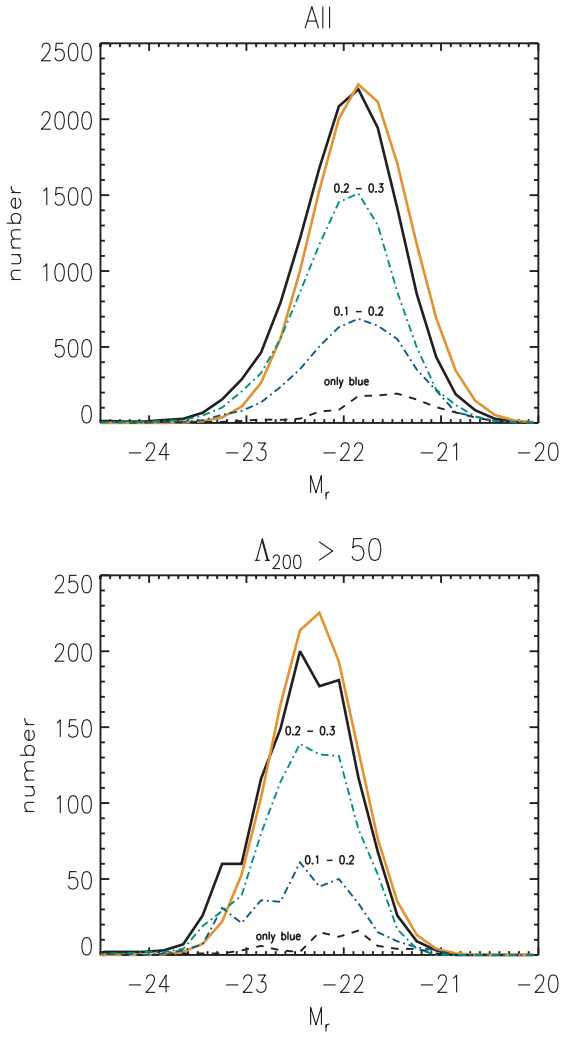

Figure 7. Upper panel: solid thick line – luminosity distribution in the r band for BCGs in the redshift range [0.1, 0.3]. Lighter thick line: Gaussian distribution with mean equal to the average of the above distribution and $\sigma = 0.5$ mag. The function for *blue* BCGs (dashed line) and the subsets of all BCGs divided into two redshift bins (dot–dashed lines) are also shown. Lower panel: as above, but only for rich clusters ($\Lambda_{200} > 50$).

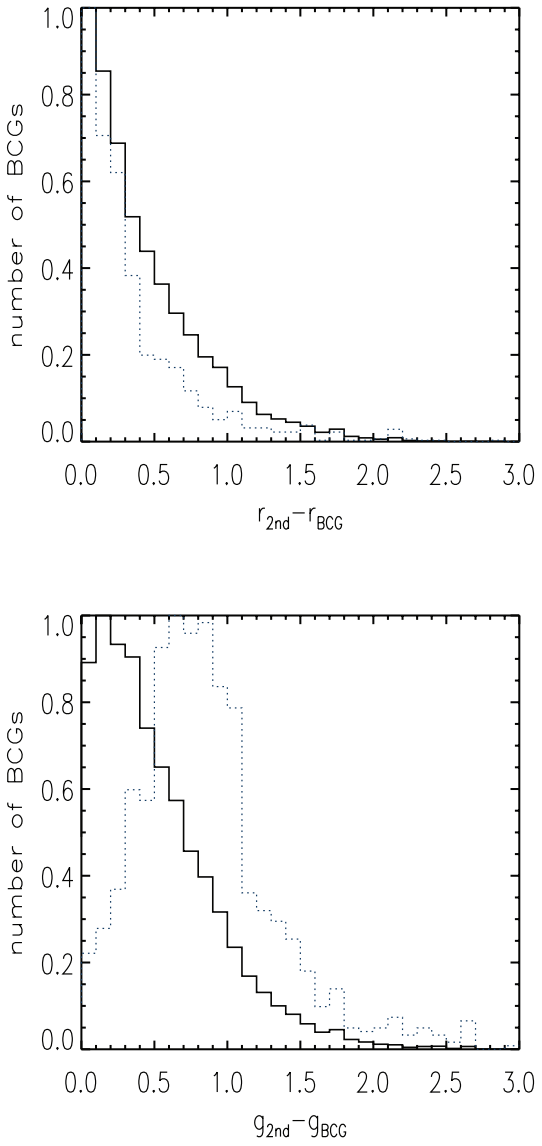

Figure 8. Distribution of galaxies dominance in r and g band. The histogram for blue BCGs is given by a dashed line.

in Fig. 8. The curve is strongly asymmetric and the galaxies tend to cluster towards very small values for the dominance. To quantify the asymmetry, we note that the average dominance in the redshift range 0.1–0.2 is 0.5 mag, which is larger than the median value (0.3 mag). The former value is inconsistent with the average given by Loh & Strauss (2006).[4] Also a standard 1σ dispersion (0.4 mag) and the mild decrease of the median dominance with redshift (0.35 mag for $z = [0.1,0.2]$, 0.3 mag for $z = [0.2,0.3]$) are in agreement with their findings. Given the asymmetry of the distribution, a more accurate estimate of the width can be given by the half width at half-maximum, which is roughly a factor of 2 smaller than the standard deviation. In the upper panel of Fig. 9, we show the distribution of galaxies in the cluster richness – dominance plane. As expected from other studies (e.g. Loh & Strauss 2006), poorer systems exhibit a larger dominance than richer clusters in that the median dominance is 0.32 and 0.25 for clusters with $\Lambda_{200} < 30$ and $\Lambda_{200} > 50$, respectively. In the former systems, the BCG, albeit less luminous, contributes a larger fraction of the total light than in the latter. In rich clusters, instead, the fraction of the total light coming from the BCG is much smaller and such a difference can tell us something on the path that lead to the formation of the BCG (e.g. Lin & Mohr 2004).

In particular, the dominance as a function of position, richness as well as the luminosity of the brightest and second brightest galaxies as a function of the dominance are very promising tools to constrain galaxy formation models and to discriminate among apparently similar recipes for the BCG star formation history (Smith et al. 2010; Skibba et al. 2011).

Finally, in the lower panel of Fig. 9 we investigate the effect of the dominance on the first ranked galaxy *blueness*, quantified in terms of the offset in magnitude from the red sequence at the galaxy redshift. No significant trends are found, except for the fact that cluster with low dominance are much more abundant than clusters where $r_{2nd} - r_{1st}$ exceeds 1 mag. When looking at the total distribution (dashed line in Fig. 8) in the r-band dominance values, the blue BCGs show

[4] Note that a direct comparison cannot be made, since they focused only on the LRGs and their neighbouring 'fields'.

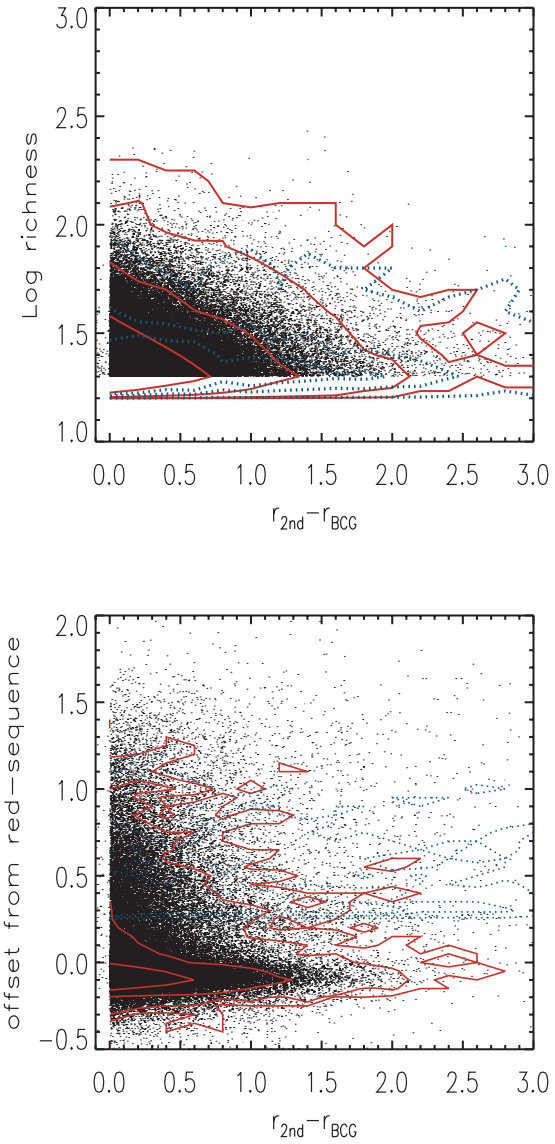

Figure 9. Upper panel: distribution of galaxies in the cluster richness versus first ranked BCG dominance plane. Lower panel: distribution of galaxies in the offset from the red sequence versus BCG dominance plane. The blue BCGs are presented with dotted contours. The numbers give the actual number of galaxies within that contour.

a somehow sharper decline, but an equally extended tail. In the g band, instead, the dominance of blue galaxies clusters around the value of $\sim$0.7 mag. This means that the blue colour of the BCG is coming from a brighter than average g-band magnitude, rather than a fainter r-band magnitude.

6 A COMPARISON WITH MAXBCG BCGs

The presence of blue BCGs is an important feature of the Szabo et al. cluster catalogue. Hence, it is important to present a quantitative comparison with a widely used catalogue as maxBCG (Koester et al. 2007) based on a strict colour selection. We briefly remind here that our BCG is defined as the brightest galaxy in the r band that likely belongs to a cluster, even though it does not necessarily sit at the cluster centre. On the other hand, the maxBCG algorithm

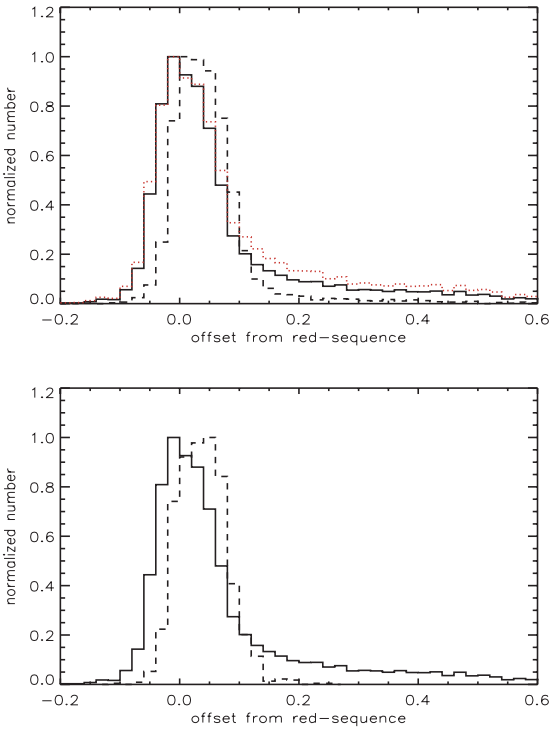

Figure 10. Upper panel: offset (mag) from $g-r$ colour–magnitude relation for all our BCGs (solid line) and those that are in clusters in common with maxBCG (dashed; see text) and those that are not (dotted line). Lower panel: offset (mag) from $g-r$ colour–magnitude relation for all our BCGs (solid line, as in the other panel) versus the offset from the colour–magnitude relation of maxBCG BCGs that belong to our clusters but that do not coincide with our BCG (dashed line).

requires a red[5] and bright galaxy and at least other 10 red and less luminous galaxies within $\sim$1 Mpc to identify a cluster. The seed galaxy is hence the BCG and the central galaxy at the same time. The cross-matching between the two catalogues has been done by searching for maxBCG BCGs that are also one of three brightest galaxies in one of our clusters. In particular, we find that more than 4300 maxBCG are in the entire Szabo et al. BCG sample. In the majority of the cases, there is a one-to-one correspondence, in the sense that only one maxBCG BCG belongs to a Szabo et al. cluster. We define these clusters as those that match the maxBCG catalogue. For a more thorough description of the matching procedure and a complete analysis of the outcome, we refer to Szabo et al. paper.

In the upper panel of Fig. 10, we show the distribution in the offset in magnitudes from the average $g-r$ colour for all our BCGs (solid line) and those that are in clusters in common with maxBCG[6] (dashed line) as well as those that are not in common (dotted line). Note that the comparison has been made by taking only Szabo et al. BCG in the sky regions where SDSS DR6 and DR5 (on which maxBCG is based) overlap and in the redshift range 0.1–0.3. We display normalized histograms in order to emphasize the tail at positive (blue) offsets in our BCGs. As expected from the maxBCG

[5] We refer to Koester et al. (2007) for the actual colour cuts; here it suffices to say that the criterion is such that the galaxy colours are within the dashed lines of Fig. 4.

[6] Note that the fact that a fraction of our clusters matches maxBCG clusters does not imply that our first ranked BCG in these clusters always coincides with the BCG of the maxBCG catalogue.

algorithm, the colours of maxBCG BCGs that also are BCGs for our clusters do not differ from those of maxBCG BCGs that belong to our clusters without being the brightest member. The distribution of our BCGs, instead, shows a more evident tail, because clusters that do not have a maxBCG counterpart tend to be poor systems (see Szabo et al. 2011), where the fraction of blue BCG is somehow larger (see above). The offset distribution for the galaxy that Szabo et al. classify as first ranked BCG in a given cluster and that for the BCGs selected according to the maxBCG method basically coincides but for the tail with blue galaxies. Therefore, in clusters that Szabo et al. and maxBCG share, the BCG selection is almost identical. In 7 per cent of the cases, maxBCG miss the brightest object because it is more than 0.3 mag away from the red sequence. However, differences are found already at 0.2 mag away from the red sequence. Such a fraction (7 per cent) is close to the fraction of blue BCG in clusters with richness >50 (see above), and it is a sensible value because most of our matches with maxBCG clusters are in the high-richness regime (see Szabo et al. 2011). The fraction is also higher than the chance probability (∼1–2 per cent, see above) of finding a relatively bright blue outliers in the cluster central regions. Since we know that the galaxy classified as BCG by Koester et al. (2007) is still one of the brightest (but not our first ranked) galaxies in our clusters, this means that maxBCG uses the second or the third brightest galaxy as seed for their clusters. Indeed, in the lower panel of Fig. 10 we plot the offset distribution for all our BCGs (solid line, as in the other panel) versus the offset from the colour–magnitude relation of maxBCG BCGs that belong to our clusters but that do not coincide with our BCG (dashed line).

A caveat is that, in order to make the comparison on a the same 'frame', we used colours and 'model' magnitudes for maxBCG BCG as provided by the SDSS DR6. Since the original maxBCG catalogue has been built from the SDSS DR5, using 'cmodel' magnitudes and different photometric redshift estimator (and hence different *k*-corrections), the exercise presented here does not provide a colour characterization of maxBCG BCGs in a strict sense.

On the basis of the maxBCG BCG colour alone, instead, we cannot explain why a fair number of maxBCG clusters is not matched by us. As shown by Szabo et al., the differing completeness above a given richness and the differing definition of richness between the two catalogues hamper a 1:1 matching. Also, we cannot exclude that we include groups where the BCGs are spirals.

7 BCGS IN X-RAY CLUSTERS

After presenting the general characteristics in terms of optical colours of the Szabo et al. BCG catalogue, we discuss one application. To this aim, we also augment the available data per each cluster/BCG by cross-matching with catalogues at other wavelengths.

Bildfell et al. (2008) found that the presence of optical blue cores in 25 per cent of its BCG sample is directly linked to the X-ray excess of the host clusters. Moreover, the position of these BCGs coincides with the peak in X-ray emission. Their interpretation is that the recent star formation in BCGs is associated with the balance between heating and cooling in the ICM in the sense that the clusters that are actively cooling are forming stars in their BCGs. The aim of this section is to confirm the results of Bildfell et al. (2008) and show how our BCG catalogue can be successfully exploited for studies of X-ray clusters and ICM properties. For this purpose, we use the entire catalogue of (first ranked) BCGs from Szabo et al., without any redshift limit.

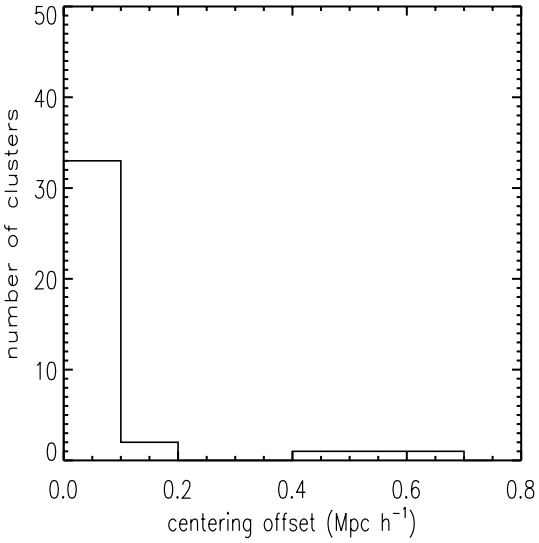

Figure 11. Positional offset between the BCG and the cluster X-ray centre for clusters in common with the ACCEPT sample.

Following Pipino et al. (2009a), we make use of the NUV − *r* colour that is more sensitive to the recent star formation than the *g* − *r* colour. Hence, we cross-matched the entire BCG sample with publicly available UV photometry from the GR4 and GR5 data release of the *GALEX* mission (Martin et al. 2005), and we find a counterpart for our entire sample of BCGs in roughly one-third of the cases. In particular, we retrieved data by means of the cross-matched GALEX GR4+GR5 – SDSS catalogue available in the GALEX archive. The positional matching, performed within 5 arcsec, returns nearly 5000 objects.

We make use of the publicly available data made possible by the ACCEPT project (Cavagnolo et al. 2009). The catalogue comprises 239 galaxy clusters with accurate temperature, density, entropy and pressure profiles reduced in a homogeneous way from public *Chandra* data. The catalogue covers the temperature range 1–20 keV with redshifts ranging from 0.05 to 0.89. We refer to Cavagnolo et al. (2009, and references therein) for details on the data reduction and further catalogue specifics. Here we note that their catalogue is neither flux-limited nor volume-limited. The matching procedure is similar to what done in Section 2.4, however a more detailed scrutiny is required. In the first place, in order to maximize the number of matches, we do not limit the analysis to BCGs in the redshift range 0.1–0.3. We discard matches that have a difference in redshift larger than 0.03 if the galaxy spectroscopic redshift is available, 0.1 otherwise.[7] In this latter case, however, we further check that the galaxies are associated to the clusters. In particular, we visually inspect the SDSS images in order to study the position of the galaxy in relation to the literature position of the X-ray cluster. In practice, the match is rejected when a clear visual overdensity of galaxies is found around the literature X-ray cluster position *but* the alleged BCG is instead isolated and more distant.

Such a procedure returns 38 matches of which 35 within 200 kpc from the cluster centres (Fig. 11). This is a well-known properties of BCGs, i.e. they are typically located within few arcseconds from the cluster centres. Pipino et al. (2009a) showed that ICM cooling time and UV–optical colour of the galaxies are connected. Therefore, in

[7] This is required because bluer galaxies sometimes have an overestimated photometric redshift.

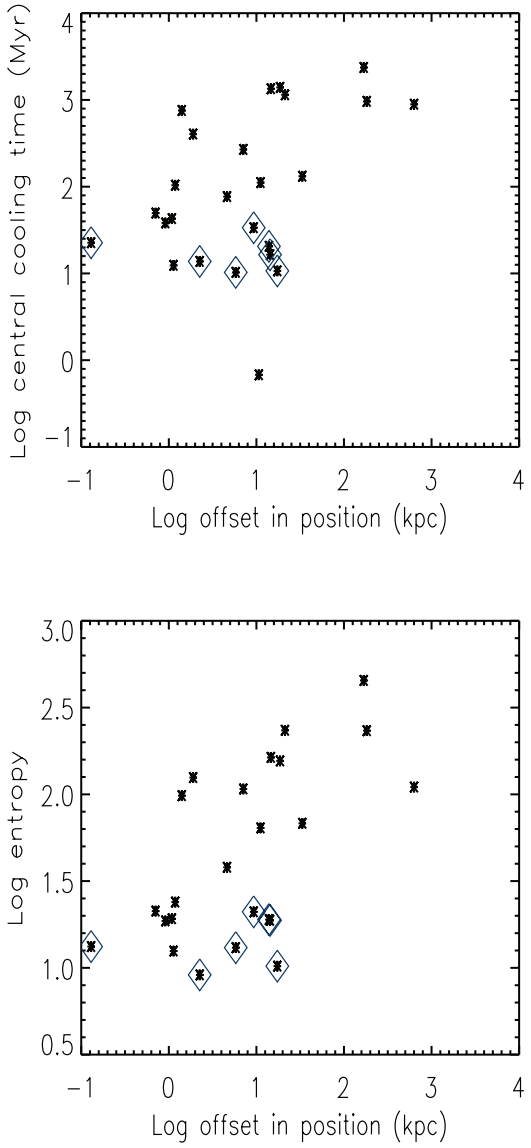

Figure 12. Cluster cooling time (upper panel) and entropy (lower panel) versus BCG's offset from the cluster centre. Symbols as in the previous figure. NUV blue (i.e. NUV $- r < 5$) BCGs are hosted by cluster with short cooling times and are at low distances from the cluster centre.

the following figures only galaxies with UV detections are shown. This decreases the sample down to 24 objects.

Here we are in the position of showing that the conclusion of Bildfell et al. is supported by the analysis of the cooling times [Fig. 12, upper panel, calculated according to equation (9) of Cavagnolo et al.] and entropy (Fig. 12, lower panel) as provided by Cavagnolo et al. (2009). A simple two-dimensional Kolmogorov–Smirnov (KS) statistical test yields ∼4 per cent (cooling time) and ∼14 per cent (entropy) probability of the NUV–optical blue BCGs and the red BCGs samples being drawn from the same distribution. Therefore, we can confirm Bildfell et al. (2008) results that a fraction of blue BCGs can be explained by cluster centres where cooling flows supply cold gas for star formation. Namely, from Fig. 13 we can see that BCGs featuring NUV $- r < 5$ reside in clusters with entropies below 30 keV cm^{-2}.

In a companion paper (Pipino & Pierpaoli 2010), we further link the presence of a cooling flow (and hence the likely presence of a blue BCG) with an enhanced SZ (Sunyaev & Zeldovich 1970) signal in order to study the bias induced in SZ-based cluster catalogues. Finally, a more general comparison of our cluster catalogue with nearly 1000 clusters observed in the X-rays at a lower spatial resolution and available in the literature is presented in the main catalogue paper (Szabo et al. 2011), where the correlation between richness and relevant quantities such as L_X and T_X is made.

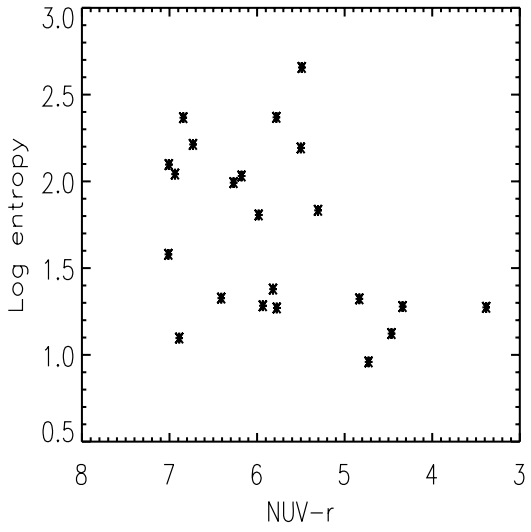

Figure 13. Cluster excess entropy versus BCG's NUV $- r$ colour for clusters in common with ACCEPT.

8 CONCLUSIONS

In this paper we characterize in terms of magnitude and colours a subsample of more than 14 300 BCGs drawn from a parent catalogue of more than 220 000 galaxies in 69 000 clusters based on the matched filter method (Kepner et al. 1999; Dong et al. 2008) applied to the SDSS DR6 (Szabo et al. 2011).

In agreement with previous works, the BCG luminosity is found to a have a redshift evolution broadly consistent with pure 'ageing' of the galaxies. Richer clusters tend to have brighter BCGs, however less *dominant* than in poorer systems. At face value, 4–9 per cent of our BCGs are at least 0.3 mag bluer in the $g - r$ colour than the red sequence at their given redshift, whereas the estimated contamination due to blue intervening galaxies is only 1–2 per cent. Such a fraction does not change if we restrict ourselves to clusters with richness above 30, and decreases above a richness of 50. In terms of redshift evolution, the overall blue fraction goes from ∼5 per cent in the redshift range 0.1–0.2 to ∼10 per cent in the redshift bin 0.2–0.3. A preliminary morphological study suggests that the increase in the blue fraction at lower richnesses has a contribution for the increase in the fraction of spiral galaxies. Therefore, we suggest a cut at richness of a least 50 (or alternatively $M_r < -22.5$ mag) if one wants to focus only on early-type galaxies. Our conservative estimate of the blue fraction in rich cluster and for galaxies with spectroscopic redshift is 1–6 per cent (99.6 per cent confidence interval).

We show that a colour selection based on the $g - r$ red sequence or on a cut at colour $u - r > 2.2$ can lead to missing the majority of such blue BCGs.

The fraction of blue BCGs is in broad agreement with previous works (e.g. Crawford et al. 1999; Edwards et al. 2007; Bildfell et al. 2008) which showed that about one-quarter of BCGs show emission lines and optical blue cores associated with recent star formation;

only a smaller fraction has the star formation extended (in time and space) enough to make their total colour blue.

We compare the colours of our BCGs in clusters in common with the maxBCGs (Koester et al. 2007) catalogue. In 7 per cent of the cases, maxBCG miss the brightest object in the Szabo et al. catalogue because it is more than 0.3 mag away from the red sequence. In this cases, the galaxy classified as BCG by Koester et al. (2007) is still one of the brightest (but not our first ranked) galaxies in our clusters; this means that maxBCG uses the second or the third brightest galaxy as seed for their clusters. It is important to stress that such a difference is not enough to explain the differences between the AMF and the maxBCG catalogues (see Szabo et al. 2011).

We also show one interesting applications of the Szabo et al. BCG catalogue. We cross-match our catalogue with the ACCEPT cluster sample (Cavagnolo et al. 2009), where accurate temperature, density and entropy profiles of the ICM can be found. We find that blue BCGs tend to be in clusters with low entropy and short cooling times. That is, the blue light is presumably associated to gas feeding of recent star formation by cooling flows (Bildfell et al. 2008).

ACKNOWLEDGMENTS

The authors thank the referee for the careful reading and many insightful comments that greatly improved the paper. AP wishes to thank S. Ameglio for many enlightening discussions, and E. Cameron, L. Edwards, J. Gunn and M. Rich for useful comments.

AP, TS and EP acknowledge support from NSF grant AST-0649899. EP is also supported by NASA grant NNX07AH59G and JPL-Planck subcontract 1290790, and thanks the Aspen Center for Physics. SMMacK acknowledges support from NSF grant NSF-PHY 0850501.

This research has made use of the SIMBAD data base, operated at CDS, Strasbourg, France; the X-Rays Clusters Database (BAX), which is operated by the Laboratoire d'Astrophysique de Tarbes-Toulouse (LATT), under contract with the Centre National d'Etudes Spatiales (CNES); the NASA/IPAC Extragalactic Database (NED) which is operated by the Jet Propulsion Laboratory, California Institute of Technology, under contract with the National Aeronautics and Space Administration. Data presented in this paper were obtained from the Multimission Archive at the Space Telescope Science Institute (MAST). STScI is operated by the Association of Universities for Research in Astronomy, Inc., under NASA contract NAS5-26555. Support for MAST for non-*HST* data is provided by the NASA Office of Space Science via grant NAG5-7584 and by other grants and contracts.

GALEX is a NASA Small Explorer, launched in 2003 April, developed in cooperation with the Centre National d'Etudes Spatiales of France and the Korean Ministry of Science and Technology.

Funding for the SDSS and SDSS-II has been provided by the Alfred P. Sloan Foundation, the Participating Institutions, the National Science Foundation, the US Department of Energy, the National Aeronautics and Space Administration, the Japanese Monbukagakusho, the Max Planck Society and the Higher Education Funding Council for England. The SDSS website is http://www.sdss.org/.

REFERENCES

Adelman-McCarthy J. K. et al., 2008, ApJS, 175, 297
Baldry I. K., Glazebrook K., Brinkmann J., Ivezic Z., Lupton R. H., Nichol R. C., Szalay A. S., 2004, ApJ, 600, 681
Bernardi M., Hyde J. B., Sheth R. K., Miller C. J., Nichol R. C., 2007, AJ, 133, 1741
Bernardi M., Hyde J. B., Fritz A., Sheth R. K., Gebhardt K., Nichol R. C., 2008, MNRAS, 391, 1191
Bildfell C., Hoekstra H., Babul A., Mahdavi A., 2008, MNRAS, 389, 1637
Blanton M. A., Roweis S., 2007, ApJ, 133, 734
Bower R. G., Lucey J. R., Ellis R. S., 1992, MNRAS, 254, 589
Cameron E., 2011, Publ. Astron. Soc. Australia, 28, 128
Cavagnolo K. W., Donahue M., Voit G. M., Sun M., 2008, ApJ, 682, 821
Cavagnolo K. W., Donahue M., Voit G. M., Sun M., 2009, ApJS, 182, 12
Choi Y.-Y., Park C., Vogeley M. S., 2007, ApJ, 658, 884
Crawford C. S., Allen S. W., Ebeling H., Edge A. C., Fabian A. C., 1999, MNRAS, 306, 857
Csabai I. et al., 2003, AJ, 125, 580
De Lucia G., Blaizot J., 2007, MNRAS, 375, 2
Dong F., Pierpaoli E., Gunn J. E., Wechsler R. H., 2008, ApJ, 676, 868
Edge A. C., 2001, MNRAS, 328, 762
Edwards L. O. V., Hudson M. J., Balogh M. L., Smith R. J., 2007, MNRAS, 379, 100
Edwards L. O. V., Robert C., Mollá M., McGee S. L., 2009, MNRAS, 396, 1953
Eisenstein D. J. et al., 2001, AJ, 122, 2267
Faber S. M., Jackson R. E., 1976, ApJ, 204, 668
Goto T., 2005, MNRAS, 360, 322
Hansen S. M., McKay T. A., Wechsler R. H., Annis J., Sheldon E. S., Kimball A., 2005, ApJ, 633, 122
Hansen S. M., Sheldon E. S., Wechsler R. H., Koester B. P., 2009, ApJ, 699, 1333
Hicks A. K., Mushotzky R., 2005, ApJ, 635, L9
Ho S., Lin Y.-T., Spergel D., Hirata C. M., 2009a, ApJ, 697, 1358
Ho S., Dedeo S., Spergel D., 2009b, preprint (arXiv:0903.2845)
Kannappan S. J., Guie J. M., Baker A. J., 2009, ApJ, 138, 579
Kepner J., Fan X., Bahcall N., Gunn J., Lupton R., Xu G., 1999, ApJ, 517, 78
Koester B. et al., 2007, ApJ, 660, 239
Larson R. B., 1974, MNRAS, 166, 585
Lin Y.-T., Mohr J. J., 2004, ApJ, 617, 879
Lin Y.-T., Mohr J., Stanford S. A., 2004, ApJ, 610, 745
Loh Y.-S., Strauss M. A., 2006, MNRAS, 366, 373
Loh Y.-S. et al., 2010, MNRAS, 410, 55
Loubser S. I., Sansom A. E., Sanchez-Blazquez P., Soechting I. K., Bromage G. E., 2008, MNRAS, 391, 1009
Martin D. C., and the GALEX Team. 2005, ApJ, 619, L1
More S., van den Bosh F. C., Cacciato M., Skibba R., Mo H. J., Yang X., 2011, MNRAS, 410, 210
Nelson A. E., Gonzalez A. H., Zaritsky D., Dalcanton J. J., 2001, ApJ, 563, 629
O'Dea C. P., Oyaizu H., Lima M., Cunha C. E., Lin H., Frieman J., 2008, ApJ, 689, 709
Pipino A., Matteucci F., 2008, A&A, 486, 763
Pipino A., Pierpaoli E., 2010, MNRAS, 404, 1603
Pipino A., D'Ercole A., Matteucci F., 2008, A&A, 484, 679
Pipino A., Kaviraj S., Bildfell C., Babul A., Hoekstra H., Silk J., 2009a, MNRAS, 395, 462
Pipino A., Devriendt J., Thomas D., Kaviraj S., Silk J., 2009b, A&A, 505, 1075
Rafferty D. A., McNamara B. R., Nulsen P. E. J., 2008, ApJ, 687, 899
Reid B. A., Spergel D. N., 2009, ApJ, 698, 143
Roche N., Bernardi M., Hyde J., 2010, MNRAS, 407, 1231
Sanchez A. G., Crocce M., Cabre A., Baugh C. M., Gaztanaga E., 2009, MNRAS, 400, 1643
Schechter P., 1976, ApJ, 203, 297
Skibba R. A., 2009, MNRAS, 392, 1467
Skibba R. A., van den Bosch F. C., Yang X., More S., Mo H., Fontanot F., 2011, MNRAS, 410, 417

Smith G. P. et al., 2010, MNRAS, 409, 169
Strateva I. et al., 2001, AJ, 122, 1861
Sunyaev R. A., Zeldovich Y. B., 1970, Comments Astrophys. Space Phys., 2, 66
Szabo T., Pierpaoli E., Dong F., Pipino A., Gunn J., 2011, ApJ, 736, 21
Tinsley B., 1980, ApJ, 241, 41
von der Linden A., Best P. N., Kauffmann G., White S. D. M., 2007, MNRAS, 379, 867
Whiley I. M. et al., 2008, MNRAS, 387, 1253

This paper has been typeset from a TEX/LATEX file prepared by the author.